

# Detecting filaments in the ultra-high energy cosmic ray distribution

Diego Harari\*, Silvia Mollerach<sup>†</sup> and Esteban Roulet<sup>‡</sup>  
 CONICET, Centro Atómico Bariloche,  
 Av. Bustillo 9500, Bariloche, 8400, Argentina.

June 27, 2018

## Abstract

We propose and test new statistical tools to study the distribution of cosmic rays based on the use of the Minimal Spanning Tree. The method described is particularly sensitive to filamentary structures, as those expected to arise from strong sources of charged cosmic rays which get deflected by intervening magnetic fields. We also test the method with data available from the AGASA and SUGAR surface detector arrays.

## 1 Introduction

The search for cosmic rays (CRs) localized excess fluxes is of utmost importance in order to identify their sources and in this way start to unravel the origin of these mysterious particles. At the highest energies at which CRs are observed,  $E > 10$  EeV (where  $1 \text{ EeV} \equiv 10^{18} \text{ eV}$ ), it is expected that charged particle trajectories straighten up and hence CR astronomy should become feasible.

The main statistical tool that has been used to search for possible sources among the few highest energy events observed, e.g. by AGASA or HiRes, has been the autocorrelation function, which was applied to quantify the abundance of multiplets appearing at small angular scales (such as the excess of doublets and triplets found by AGASA within  $2.5^\circ$  and above 40 EeV[1], but not confirmed by HiRes[2]). On the other hand, when the event statistics is high (as for lower energy thresholds), the search for overdensities with respect to isotropic expectations on specific angular scales has been used to identify possible excesses, such as those reported by AGASA

---

\*Email: harari@cab.cnea.gov.ar

<sup>†</sup>Email: mollerach@cab.cnea.gov.ar

<sup>‡</sup>Email: roulet@cab.cnea.gov.ar

[3] and SUGAR [4] for EeV energies near the location of the galactic center (but not confirmed by Auger [5]).

In this paper we propose the use of an alternative tool, the Minimal Spanning Tree (MST), to search for possible CR sources. This approach is particularly sensitive to elongated structures in the distribution of arrival directions and is well suited for the analysis of samples of events with statistics from few tens up to several thousands of events, and hence should be specially useful for the search and identification of the first candidate sources in the new generation of high statistics UHECR experiments, such as Auger.

Cosmic rays coming from a given source suffer an energy dependent deflection due to the magnetic fields present along their trajectories. The typical deflection produced by a regular component of the magnetic field decreases with increasing energy and after traversing a distance  $L$  in a magnetic field  $\mathbf{B}$  is given by

$$\delta \simeq 5^\circ \frac{10 \text{ EeV}}{E/Z} \left| \int_0^L \frac{d\mathbf{x}}{\text{kpc}} \times \frac{\mathbf{B}}{\mu\text{G}} \right|, \quad (1)$$

and hence the typical strength of the regular galactic magnetic field (few  $\mu\text{G}$ ), which is coherent over lengths of a few kpc, can induce deflections of order ten degrees for  $E/Z = 10 \text{ EeV}$ , depending on the CR arrival direction ( $Z$  is the charge of the CR). The turbulent component of the magnetic field is expected to produce smaller overall deflections due to the reduced scale of the field coherence length, adding a randomly oriented deflection to the smoother change with energy in the source apparent position caused by the regular field [6]. The combined effect of both components is expected to generally produce elongated and diffused images of the cosmic ray sources. The intergalactic random magnetic fields, which although are expected to have reduced strength ( $\leq 10^{-9}\text{G}$ ) can have large coherence lengths ( $\sim \text{Mpc}$ ) and may act over long distances, can also further diffuse the images of point-like CR sources, but the size of the induced deflections is currently under debate [7, 8].

The usual statistical tools to look for small scale clustering in the CR angular distribution, like the autocorrelation function mentioned before, may not be the optimal ones to look for the expected filamentary-like structures. The alternative strategy that we propose uses the MST, which is a unique network associated to any distribution of points that connects all the points, without forming closed loops, and having the smallest total length. Its main advantage is that it picks out the dominant pattern of connectedness in a manner that emphasizes the linear intrinsic structures. Because of this, it has successfully been used to study the filamentarity in the large scale distribution of galaxies [9, 10]. We here adapt the method to the analysis of cosmic ray data and introduce the statistics that can optimize the search for localized excesses.

To construct the MST for a given set of points (e.g. the CR arrival directions in some energy range) one possibility is just to start from any point in the set and find its closest neighbor. The segment linking this pair of points constitutes the first

edge of the tree. Next, one looks among the remaining points for that one which is the closest to any of the points that are already in the tree, and adds the new edge connecting these points to the tree. This procedure is repeated until all the points get connected. Then, for a set of  $N$  points, the tree is formed by  $N - 1$  edges, and it is unique if the distances between all the points are different. This also means that the tree is independent from the starting point chosen.

There are various operations which can be performed on a tree in order to enhance its sensitivity to study a particular property, the most useful being pruning and separating. In a pruned tree branches are removed preserving the main skeleton. In a separated tree edges exceeding some fixed cutoff (which is usually fixed in terms of the mean edge length) are removed. This operation tends to remove accidental linkages among independent structures, and we will implement it in order to isolate the most relevant structures that may be related to individual cosmic ray sources. Pruning instead is more important to reveal a possible global structure in the pattern of arrival directions and we will not implement it here.

Different statistical properties of the MST can be analyzed to pick the different characteristics of a given distribution of points. The simplest one is the total length of the tree. Other possibilities include the frequency distribution of edge lengths measured in terms of the mean edge length, for which a sample presenting localized structures shows an excess of segments with lengths shorter than the mean and a larger tail of segments with longer lengths as compared to a random distribution of points [9] (notice that there is hence some compensation in the net effects on the average edge length in these cases).

In this work we adapt the MST technique to account for the effects of the non-uniform exposure associated to different directions in the sky that is typical in CR experiments. We do that in section 2 by introducing a tree built on the basis of rescaled angular distances, and by so doing the results obtained are not biased towards high exposure regions. We propose in section 3 the use of a different statistics which is specially suited to look for isolated filamentary structures superimposed to an homogeneous background. The main idea is to study the distribution of the multiplicities (i.e. the number of points) of the disjoint pieces of the separated tree after having cut all the edges with size greater than the mean edge length. We also introduce in section 3 the concept of compact multiplicity, which allows to give a measure of how dense the separated event groups are, what helps then to rank the clusters in a more meaningful way. This procedure permits also to naturally select the groups of events that are most probably associated with the strongest sources.

In section 4 we test the method with simulated structures superimposed to an isotropic background, showing that these can be efficiently recovered, while in section 5 we apply the technique to the available AGASA and SUGAR data.

## 2 The standard MST and the exposure weighted one

In order to develop the procedure in detail and test the results for the particular problem of the observed distribution of cosmic rays, we will use simulated data sets in which the partial sky coverage and the non-uniform exposure of the observatory is taken into account, assuming for definiteness an experiment located at the latitude of the Pierre Auger Observatory ( $b = -35.2^\circ$ ) and with maximum observed zenith angles of  $60^\circ$ .

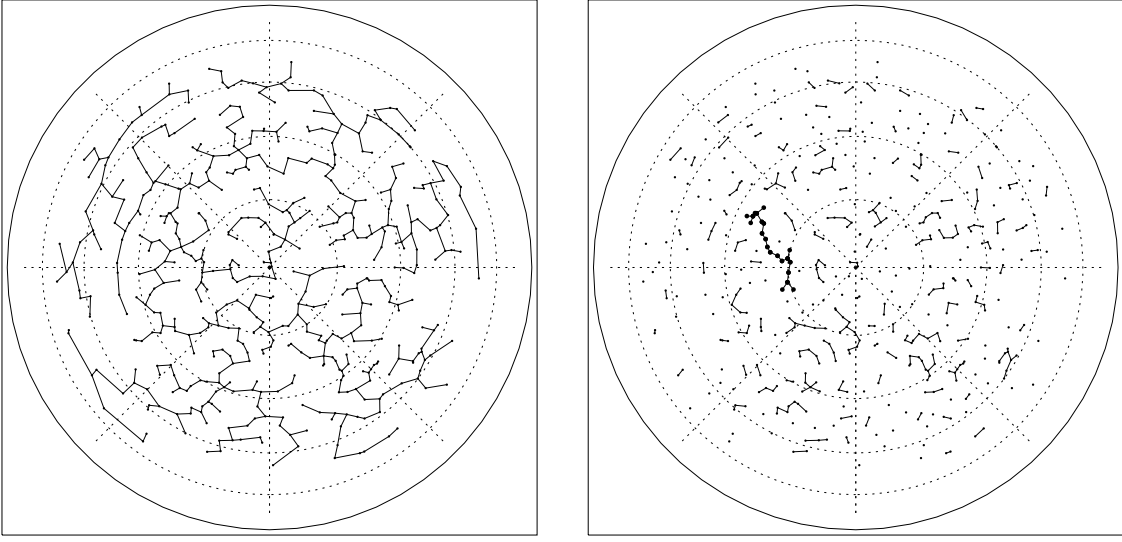


Figure 1: Maps with 500 simulated isotropic events and the standard MSTs. The left panel shows the whole tree while the right panel shows the separated one, in which the edges larger than the average separation among events are discarded. Big dots indicate the largest multiplicity object. The grid has a spacing of  $30^\circ$  in declination.

In the left panel of fig. 1 we display with dots a sample of 500 random isotropic events generated according to the geometric exposure corresponding to full acceptance for such an experiment [11]. The map is an equal area projection centered in the southern celestial pole.

The MST, built by joining points according to their angular distance in the sky through the approach described before, consists of all the edges depicted. They give a unique structure going through all points, having no loops and minimal length.

In the right panel of fig. 1 we display instead the separated tree, in which all edges larger than the mean edge length of the original tree shown in the left panel are removed, and hence only the events at distances smaller than average get associated into clusters. This naturally selects the regions where the density of events

is enhanced, and identifies the corresponding arrival directions. The largest multiplicity cluster for this simulation contains 21 events, indicated by large dots in the plot.

One problem of this simple approach is that since the exposure depends on declination (we are assuming for simplicity that it is uniform in right ascension, as is approximately the case for surface detectors running for long periods of time), the expected average distance among events also depends on declination. Hence, having separated the tree at a common distance favors the formation of the biggest clusters in the regions where the exposure is larger (in this case, at declinations towards the south of the latitude of the detector), and not necessarily where the strongest sources could be located.

We will hence implement a different approach by which the tree is built by comparing not directly the actual angular distances among events, but instead the distances rescaled by the square root of the exposure (taken e.g. at the mean declination of the two events being compared<sup>1</sup>). In this way, when separating the tree by the average rescaled distance, the events associated in objects will really have neighbors at less than the average expected separation in that direction, and no bias towards high exposure regions will be introduced.

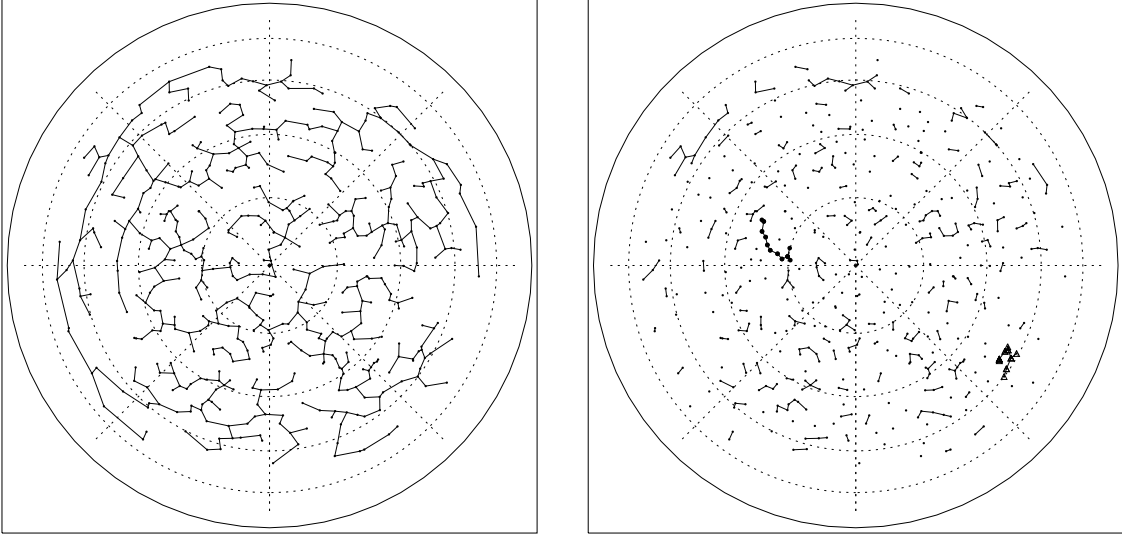


Figure 2: Maps with 500 simulated isotropic events (the same as in Fig. 1) and the exposed weighted MSTs. On the left is the whole tree while on the right the separated one.

The left panel of fig. 2 shows the new tree just discussed with the same events as in fig. 1, while the right panel depicts the associated separated tree. We see that

---

<sup>1</sup>The results are almost insensitive to the way in which this is implemented, and essentially the same is obtained by taking e.g. the square root of the average exposure, or the average of the square roots of the exposure, etc.

now the large multiplicity objects are distributed more uniformly in declination (compare with fig. 1). The object with the largest multiplicity, indicated with large dots, turns out now to be different.

Notice from the trees in the left panels of figs. 1 and 2 that many events near the border of the region observed (at declination  $\delta \simeq 25^\circ$ ) are linked among themselves. This border effect is easy to understand thinking for instance on how the tree of a large region is affected if this region is divided into two. Many events near the border between the two sub-regions, which before the division were linked to an event in the other sub-region, will now have to be linked to a different nearby event in the same subregion. Hence, many links among events near the border result. However, these new links are usually larger than average, and hence one doesn't find any bias towards the borders in the separated trees of the right panels of figs. 1 and 2. In those figures there is in addition a visual effect associated to the polar projection used, which tends to induce azimuthal elongations far from the South pole, but this has no connection with the genuine effect discussed above.

### 3 Standard multiplicity and compact multiplicity

A further relevant issue for the identification of event clusters associated to potential strong CR sources is the compactness of the separated objects of the tree. It is indeed clear that if two objects have similar multiplicities, the one for which the events are closer together (using the exposure weighted angular distance introduced in the previous section) will be the more interesting one. Moreover, even clusters of low multiplicity may be quite relevant if the events are sufficiently nearby, such as was the case for the doublets and triplets observed by AGASA. We will hence introduce the concept of *compact multiplicity*  $\hat{N}_i$ , which is just the multiplicity  $N_i$  of the separated tree object, divided by the average scaled angular distance  $\bar{\alpha}_i$  of that object (in units of the average  $\bar{\alpha}$  for the whole tree before separation), i.e.

$$\hat{N}_i = N_i \frac{\bar{\alpha}}{\bar{\alpha}_i}, \quad (2)$$

with

$$\bar{\alpha}_i \equiv \frac{1}{N_i - 1} \sum_{j=1}^{N_i-1} \alpha_j. \quad (3)$$

Here the sum is over the  $N_i - 1$  edges in the object and  $\alpha_j$  is the scaled angular distance of the edge<sup>2</sup>. Notice that the average separation of the events within objects,  $\bar{\alpha}_i$ , is always smaller than the average separation  $\bar{\alpha}$ , and hence  $\hat{N}_i > N_i$ .

For instance, the object with the largest compact multiplicity in the isotropic simulation of figs. 1-2 is the one indicated with triangles in fig. 2 (right panel). It

---

<sup>2</sup>In the case in which the angular extent of the object  $\sum_{j=1}^{N_i-1} \alpha_j$  turns out be smaller than the rescaled angular resolution of the experiment,  $\alpha_{res}$ , we adopt  $\alpha_i = \alpha_{res}/(N_i - 1)$  in order not to artificially overweight those clusters.

has a multiplicity  $N_i = 9$ , while  $\hat{N}_i = 19.1$ , since the average separation between events in that object is  $\sim 0.47$  of the global average separation.

## 4 Identifying CR sources

Since the autocorrelation function  $C(\theta)$  counts the number of pairs with separation smaller than a given angle  $\theta$ , it is particularly sensitive to the presence of clusters at very small angles (much smaller than the average separation among events), for which very few pairs are expected to result from chance coincidences. This was indeed the case for the signals reported by AGASA above 40 EeV, which involved several clusters (5 doublets and one triplet) essentially at the scale of the angular resolution of the experiment,  $2.5^\circ$ , while the average separation among the 59 events of the sample was  $> 10^\circ$ .

However, since the number of pairs expected grows as  $\theta^4$  (for small  $\theta$ ), the significance of a few clusters of events with separations comparable to the mean angular separation of the events will be diluted by the large number of chance pairs normally expected at those angular scales<sup>3</sup>. On the contrary, the MST technique is well suited to identify this kind of overdense regions, since it efficiently isolates the clustered events and can hence determine that they are unusual.

To see this we show an example in which an elongated structure consisting of 10 events aligned along the equator and separated by  $5^\circ$  among each other is superimposed to isotropic simulations (with the exposure corresponding to full acceptance at the Auger latitude) with different total number of events  $N$ .

The simulated data set for a total of 500 events is shown in the left panel of fig. 3, together with the associated separated tree (using the rescaled angular distances). The largest compact multiplicity cluster, indicated with large dots, is indeed associated to the aligned events introduced by hand. In the right panel we show (solid line) the fraction of isotropic simulations leading to a cluster with compact multiplicity larger than the largest one found in the simulated data set with the elongated source, as a function of the total number of events  $N$  considered. This fraction is quite small ( $< 10^{-2}$ ) up to  $N \sim 600$ . Notice that the average separation among events is  $\sim 10^\circ/\sqrt{N/100}$ , and hence we see that the fraction is particularly small when the average separation among the events from the source is smaller than the average separation among the background events. In this example the autocorrelation function is not sensitive to the added source. For instance, at the scale of  $5^\circ$  where the autocorrelation is most sensitive to the structure put in by hand, already for a total of 70 events the fraction of simulations having larger number of pairs at that scale is  $> 10\%$ . Similarly, a blind search of overdensities in circular windows would not have been sensitive to the elongated structure introduced. It has to be

---

<sup>3</sup>An exception is when a large scale pattern, such as a dipole, is present in the data, in which case the overdense region leads to an enhancement in the observed number of pairs at large angular scales.

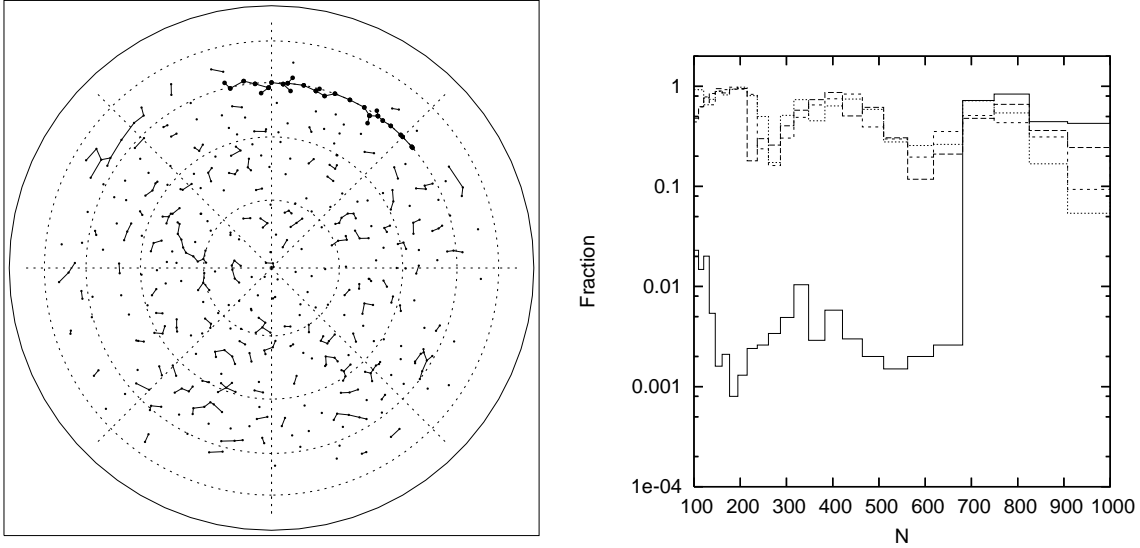


Figure 3: Left panel: map with 500 events consisting of a simulated isotropic background with the addition of a string of 10 events along the equator, separated by  $5^\circ$  one from the other. The exposure weighted separated MST is superimposed. Right panel: Fraction of isotropic simulations having a cluster with compact multiplicity larger than the data in the left panel, as a function of the total number of simulated events. Different lines correspond to the first, second, third and fourth largest multiplicity objects (in decreasing order of dash length).

noticed that both the autocorrelation and the overdensity searches, contrary to the MST, require a scan over the angular scales analyzed, besides the scan over energy that is common to all techniques.

We also show in fig. 3 (right panel) the fraction of isotropic simulations having a compact multiplicity for the second largest multiplet larger than that of the simulated data set (long dashes), and similarly for the third (medium dashes) and fourth (short dashes) largest multiplets. These kind of tests can be useful to identify if there is more than one abnormally large multiplet, which was not the case for the simulated data we used in this example.

As a second illustrative example, we show in figs. 4 plots similar to those in figs. 3 but for the case of an isotropic simulation to which we added three linear structures of 7 events each, separated by  $3^\circ$  from one event to the next. One of the structures is near the south pole, another near declinations of  $-45^\circ$  and the third one is along the equator. Although the largest multiplet in the data is not very unlikely (since a multiplet with  $\sim 7$  events is quite common for  $N > 100$ ), the other ones are quite unlikely up to  $N \sim$  few hundreds. Notice that even if only 3 sources are put in by hand, also the fourth largest multiplet is unlikely, since this one turns out in general to be the one that would have been the largest multiplicity object in the sample had we not introduced the ad hoc sources.



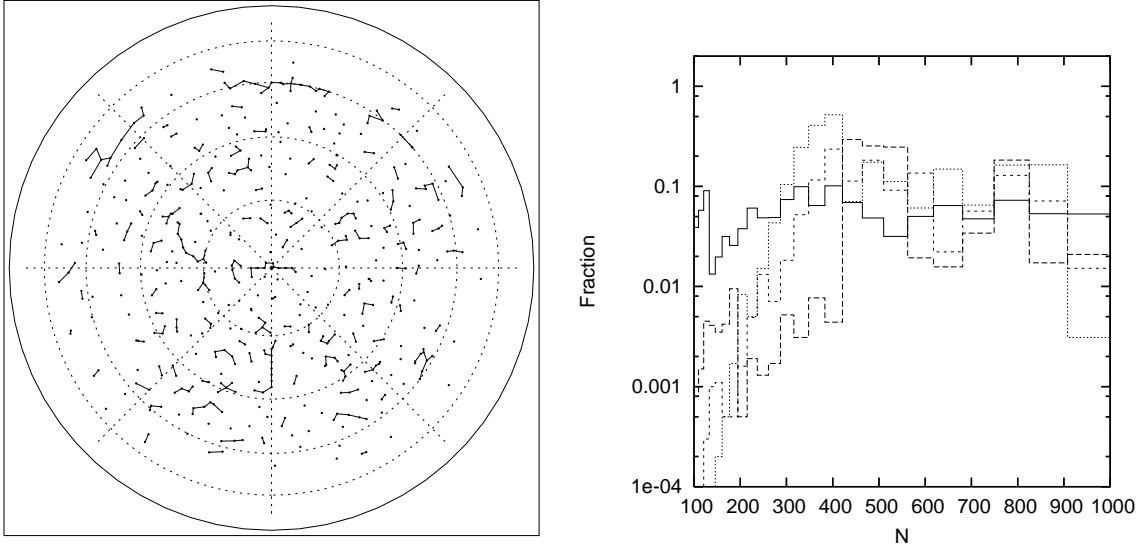


Figure 4: Same as fig. 3, but for 500 events consisting of a simulated isotropic background with the addition of three strings of 7 events, separated by  $3^\circ$  one from the other.

It is important to keep in mind that once an uncommon structure is identified by means of the MST, many detailed studies of those events can be useful. In particular, the energy spectrum of the clustered events can be of interest, and angle-energy correlations can provide information about the intervening magnetic fields or about the charge composition of the CRs, they can allow to better reconstruct the original source location, etc. [12].

## 5 AGASA and SUGAR MSTs

As an example of an application of the MST technique, we show in figs.5 the four objects with highest compact multiplicities in the separated weighted trees obtained with the 72 most energetic AGASA events [1] (with  $E > 40$  EeV and zenith angle below  $45^\circ$ ) as well as the 300 more energetic SUGAR events [13] (with zenith below  $60^\circ$ ), assuming the geometric, full-acceptance exposures at the latitudes appropriate for those experiments. None of these objects is very unlikely to occur in random isotropic realizations. The fraction of isotropic simulations leading to objects with larger compact multiplicities than the four more clustered AGASA objects are 22%, 2%, 19% and 9% respectively (note that the largest compact multiplicity object found is the well known AGASA triplet), while in the case of the SUGAR objects they are 50%, 40%, 47% and 59% respectively. No abnormally large multiplicity objects appear either in the MSTs of the SUGAR data with the 100 and 200 highest energy events.

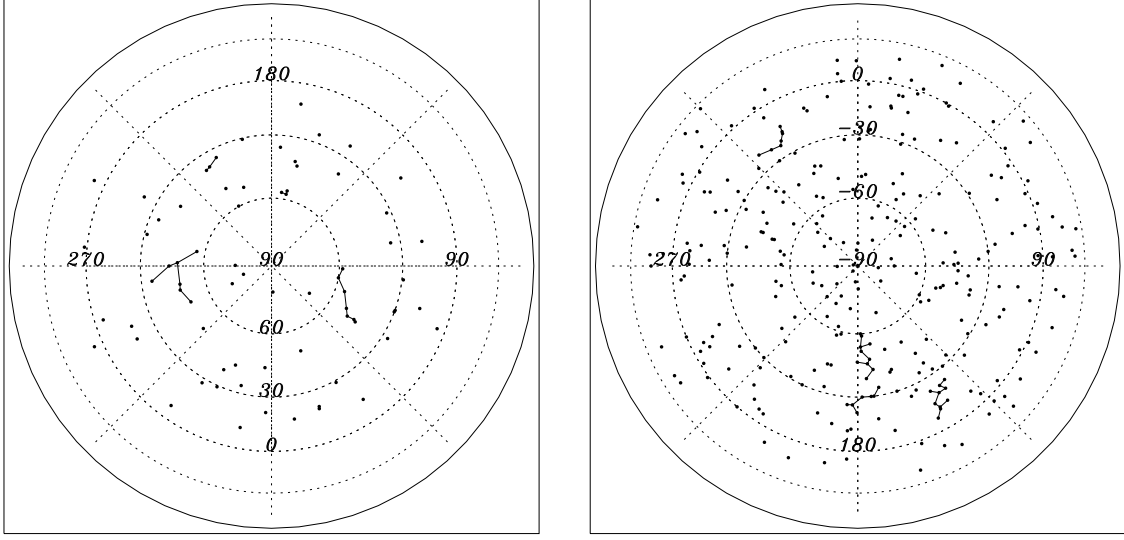


Figure 5: Four objects with highest compact multiplicities in the exposure-weighted MSTs of the 72 highest energy AGASA events (left panel, map centered in the Northern Celestial Pole) and of the 300 highest energy SUGAR events (right panel, map centered in the Southern Celestial Pole).

## 6 Conclusions

As a summary, we have shown that the MST provides a very interesting tool to search for filamentary-like structures in the distribution of CR arrival directions. We adapted the method in order to account for the effects of the non-uniform exposure typical of CR experiments. We introduced the study of the multiplicities of the separated clusters as an efficient method to identify potential sources. We further developed the concept of compact multiplicities, which allows to give larger significance to denser concentrations of events. By comparing the largest multiplicities observed in the data set under analysis with those obtained in isotropic simulations with the same exposure, it is possible to characterize how likely these configurations are and identify the events that constitute them. We illustrated the power of the method with fake data consisting of different strings of events (representing idealized strong CR sources) superimposed onto an isotropic simulated background. Although the traditionally used tools such as the autocorrelation function or the overdensity searches would have been unsensitive to those structures, the MST based technique introduced in this work was able to efficiently isolate the fake sources and show that they were unusual even in the presence of a significant number of background events. We then applied these tools to the available AGASA and SUGAR data, without finding any very significant evidence in favor of the presence of elongated structures in those datasets.

This method should be useful for the search of signals from powerful CR sources

in the next generation of large CR detectors, such as the Auger Observatory, which is near completion and already gathering very large statistics of ultra-high energy events.

## Acknowledgments

We thank support from CONICET, ANPCyT and Fundación Antorchas.

## References

- [1] M. Takeda et al., (AGASA Collaboration), *Small scale anisotropy of cosmic rays above  $10^{19}$  eV observed with the Akeno Giant Air Shower Array*, Astrophys. J. **522** (1999) 225, [astro-ph/9902239]; M. Teshima et al., (AGASA Collaboration), *The arrival direction distribution of extremely high energy cosmic rays observed by AGASA*, Proc. 28<sup>th</sup> ICRC, Tokyo (2003), 437, Universal Academy Press, Inc.
- [2] R. U. Abbasi et al., (HiRes Collaboration), *Study of small-scale anisotropy of ultra high energy cosmic rays observed in stereo by HiRes*, Astrophys. J. **610** (2004) L73, [astro-ph/0404137].
- [3] N. Hayashida et al. (AGASA Collaboration), *The anisotropy of cosmic ray arrival directions around  $10^{18}$  eV*, Astropart. Phys. **10**, 303 (1999) [arXiv:astro-ph/9807045], N. Hayashida et al. (AGASA Collaboration) ICRC 1999, Salt Lake City, OG.1.3.04, [astro-ph/9906056].
- [4] J. A. Bellido et al., *Southern hemisphere observation of a  $10^{18}$  eV cosmic ray source near the direction of the galactic center*, Astropart. Phys. **15**, 167 (2001) [astro-ph/0009039].
- [5] The Pierre Auger Collaboration, *Anisotropy studies around the galactic centre at EeV energies with Auger data*, ICRC-2005-119, [arXiv:astro-ph/0507331].
- [6] D. Harari, S. Mollerach, E. Roulet and F. Sánchez, *Lensing of ultra-high energy cosmic rays in turbulent magnetic fields*, JHEP **0203**, 045 (2002) [arXiv:astro-ph/0202362].
- [7] G. Sigl, F. Miniati and T. Ensslin, *Ultra-high energy cosmic ray probes of large scale structure and magnetic fields*, Phys. Rev. **D70** (2004) 043007, [astro-ph/0401084].
- [8] K. Dolag, D. Grasso, V. Springel and I. Tkachev, *Mapping deflections of extragalactic ultra-high energy cosmic rays in magnetohydrodynamic simulations of the local universe*, JETP Lett. **79** (2004) 583, astr0-ph/0310902.

- [9] J. D. Barrow, S. P. Bhavsar and D. H. Sonoda, *Minimal spanning trees, filaments and galaxy clustering*, Mon. Not. R. Astron. Soc. **216**,17 (1985).
- [10] R. C. Pearson and P. Coles, *Quantifying the geometry of large-scale structure*, Mon. Not. R. Astron. Soc. **272**, 231 (1995).
- [11] P. Sommers, *Cosmic Ray Anisotropy Analysis with a Full-Sky Observatory*, Astropart. Phys. **14**, 271 (2001) [arXiv:astro-ph/0004016].
- [12] D. Harari, S. Mollerach and E. Roulet, *Astrophysical magnetic field reconstruction and spectroscopy with ultra high energy cosmic rays*, JHEP **0207**, 006 (2002) [arXiv:astro-ph/0205484].
- [13] M.M. Winn et al., J. Phys. G **12**, 653 (1986); and *Catalogue of Highest Energy Cosmic Rays* No. 2, p. 68 (1986).